J Mater Sci (2010) 45:1547–1552
DOI 10.1007/s10853-009-4122-3

Synthesis of silver nanoparticles from carboxylate precursors under hydrogen pressure

Pawel Uznanski · Ewa Bryszewska

Received: 29 September 2009 / Accepted: 9 December 2009 / Published online: 29 December 2009

Abstract A direct, high yield synthesis for preparing narrow-size silver nanoparticles by decomposition of silver carboxylate precursor under H_2 pressure (3 bars) in solution is reported. The method corresponds to that for nanoparticles synthesised by thermal decomposition of carboxylic acid silver salts, but is faster, reproducible, versatile, and easier to control. Most of carboxylate groups are reprotonated upon the presence of dihydrogen and subsequent reduction of Ag^+ produces spherical particles of dimensions 4–6 nm. The IR studies indicate that aliphatic carboxylates chemisorb on the nanoparticle surface with the two oxygen atoms coordinated mostly symmetrically and forming bridging bidentate Ag–O bonds. This implies strong interactions between the surfactant and Ag nanoparticle and enhances the stability of Ag colloid. There are some sites yet, probably at vertex or facet atoms of the nanoparticle, which form linkages of chelating bidentate or ionic character. Silver particles can be additionally capped in situ either by aliphatic primary amines or thiols forming mixed carboxylate/amine or carboxylate/thiol protecting monolayer. It is demonstrated that coordination of the second ligand adjusts physicochemical properties of nanoparticles. In the dual passivating system both amine and thiol were found to be tightly bounded to the silver nanoparticle surface.

P. Uznanski (✉) · E. Bryszewska
Centre for Molecular and Macromolecular Studies, PAS,
Sienkiewicza 112, 90-363 Lodz, Poland
e-mail: puznansk@cbmm.lodz.pl

Introduction

Long alkane chain amines, thiols, carboxylic acids, and phosphine oxides were found to be very effective for stabilizing metal nanoparticles (NPs) in various solvents, not only noble metal ones [1–11] but also ruthenium [12], cobalt [13], iron [14], nickel [15]. There is limited number of metal precursors where the ligand coordinated to a metal ion forms a protective shell of nanoparticle after decomposition. The advantage of using such organometallic precursors is connected with the post-reaction cleaning procedures based on removing waste byproducts, excessive stabilizers, reducing agent, etc. Long aliphatic chain silver carboxylates are examples of precursors where capping ligands coordinated at the surface of the particles are derived from initial metal precursor [16, 17]. Ligands of the precursor act as capping tool for the formed nanoparticles. This method requires, however, high temperatures (250 °C) and longer times (several hours) due to thermal stability of the carboxylate precursor. Nakamoto and coworkers have modified the thermolytic process introducing primary or tertiary alkylamines as solvent molecules which create with silver salt an intermediate carboxylate-amine adduct [18–20]. This allowed one to decrease the temperature and time for the reduction reaction of silver atoms. Silver nanoparticles capped by alkyl carboxylates may find practical applications. After annealing they are considered as material with sufficiently high electrical conductivity to be used in printing of low-cost electronic circuits [21–24].

Although thermolysis is a powerful and well established procedure among the other large scale preparation methods of monodispersed nanoparticles [25–27], the mechanism of silver carboxylate thermal decomposition is still a matter of conjecture. Taking into account that free carboxylic acid is formed quantitatively at 250 °C in N_2 atmosphere, and

there is no evidence for CO_2 and Ag_2O products, one can assume that hydrogen atoms are formed in *statu nascendi* either by dehydrogenation of the organic moiety or by hydrolysis (water molecule bounded to the initial precursor). No evidences have been given so far for verifying such hypotheses. A question concerning the mechanism of carboxylate oxidation drove us to a trivial statement that hydrogen atoms may originate also from external source, as it is well established in organometallic chemistry.

To fabricate silver nanoparticles under mild conditions we propose in this communication to apply dihydrogen as reducing agent of metal carboxylates at elevated pressure. Although synthesis of metal nanoparticles from oraganometallic derivatives in the presence of reactive gas (CO, H_2) is well recognized for olefinic complexes (see e.g., review paper [28]) there are only a few reports on decomposition of silver precursors under a reductive atmosphere of H_2 [29–31]. This work shows that reprotonation of the carboxylate ligand of Ag^+ ion into the corresponding coordinatively inert carboxylic acid yielded nanoparticles which display optical properties analogous to that prepared by high temperature decomposition. Applying pressurized dihydrogen it is possible to change dramatically other reaction conditions such as temperature, solvent, reaction time or to introduce in situ additional capping agents. The proposed synthetic method can potentially facilitate fabrication of high quality nanoparticles. In terms of achievable particle sizes, polydispersities, and simplicity the method is comparable to that by Nakamoto [17, 19]. Concurrently, it allows to lower the temperature of the reaction and to use various solvents, both polar and non-polar ones. The other stabilizing ligands can also be employed as component of the final capping monolayer. The particles in dried form remain stable over a long period of time, and if necessary can be readily redispersed in organic solvents.

Experimental

Materials

Palmitic acid (99%), 1-hexadecylamine (99%) (HDA), 1-hexadecanethiol (99%) (HDT), silver nitrate (99%), and sodium hydroxide (98%) were purchased from Aldrich and used as received. Solvents (methanol and toluene) prior to use were distilled over CaH_2; water was triply distilled. Carboxylic acid sodium salt was prepared by adding aqueous solution of NaOH (0.72 g/4 mL) to the 0.1 M solution of palmitic acid (5.12 g/0.2 L) in hot water (80 °C). The molar amount of NaOH was 1% lower than that of the acid in order to avoid the reaction of excess alkali with $AgNO_3$. The resulting sodium carboxylate was mixed with an aqueous solution of $AgNO_3$ (1 equiv in 20 mL) and afforded white precipitate was collected, washed with water (3×) and dried at 60 °C overnight to give white solid in quantitative yield.

Characterization techniques

Electron microscope images were obtained using a Tesla instrument operating at 200 kV with samples deposited on a carbon cooper grid. FTIR spectra of the Ag NPs samples (prepared by spreading a drop of the sol in cyclohexane on Si plate and letting it dry) were run using a Nicolet 380 FT-IR spectrophotometer. UV–Vis absorption was measured in a Specord S600 diode array instrument (Analytik Jena) in the range 200–1000 nm, with a resolution of 0.5 nm. Differential scanning calorimetry (DSC) and thermogravimetry (TG) were recorded in the presence of air on a DSC 2920 and TGA 2950 (TA Instruments), respectively. Approximately 6.0 mg of the material was used, and the heating process was recorded at the rate of 10 °C/min. Microanalysis was performed with an Euro-Vector model 3018 instrument.

Results and discussion

Typically the reaction was conducted at 140 °C and the H_2 pressure 3 bars. Silver palmitate (2 mmol, 0.724 g) and toluene (1.5 ml) were introduced in a Fischer-Porter bottle and degassed by freeze-pump cycle. The suspension was pressurized under dihydrogen, heated by immersing into silicon oil bath and allowed to react for 15 min, during which it gradually turned yellow–brown. Under these conditions the insoluble salt slowly dissolved taking consistency of gel [32] and finally affording homogeneous dispersion of silver nanoparticles (colloid Ag-Pal). The reaction was quenched after 15 min by immersing the flask in a cold water bath and elimination of dihydrogen excess. Upon completion of the reaction the color of the solution turned into transparent yellow–brown. The reaction products comprised palmitic acid and silver-binding palmitate. The nanoparticles were isolated by precipitation with methanol (5 mL). The solvent and palmitic acid were easily removed from a Fisher-Porter reaction ampoule by a pipette, leaving the dark-blue waxy material on the flask wall. Sedimented nanoparticles were further cleaned and separated by washing out twice with methanol and air dried. Purified dark powder remained soluble in organic solvents (hexane, toluene, chloroform) even after prolonged storage in air. All other syntheses were performed using the same procedure with 2 mmol of silver palmitate, 3 bar H_2 pressure, 15 min reaction time at the temperature of 140 °C, and with either 0.1 equiv of hexadecylamine

Table 1 Elemental organic composition and silver content for three nanoparticle samples studied

Sample	Amount of added ligand	Ag content[a] (%)	Microanalysis (%)					Overall organic composition (%)
			C	H	O	N	S	
Ag-Pal	–	70.45	23.28	3.81	5.99	–	–	33.08
Ag-Pal/HDA	0.1 equiv HDA	59.32	32.73	5.57	5.99	0.28	–	44.57
Ag-Pal/HDT	0.1 equiv HDT	57.01	33.34	5.55	6.14	–	1.42	46.45

[a] The content was estimated by a thermogravimetric analysis. The dried sample was the weight of silver core with ligands. The residue weight obtained after heating a specimen to 500 °C was the amount of silver in the sample, and subsequently gave the silver fraction in nanoparticles

(sample Ag-Pal/HDA) or with 0.1 equiv of hexadecanethiol (sample Ag-Pal/HDT). In both cases the color changes occurred faster than for pure silver palmitate. Chemical elemental analyses of the vacuum dried silver NPs for C, H, N, O, and S gave an overall content of organic material 33.08, 44.57, and 46.45% for powered samples of Ag-Pal, Ag-Pal/HDA, and Ag-Pal/HDT, respectively. The silver content for all three samples was estimated from thermogravimetric analysis as the residual weight obtained after heating the specimens to 500 °C and amounted to 70.45% for Ag-Pal, 59.32% for Ag-Pal/HDA and 57.01% for Ag-Pal/HDT (Table 1).

These results show apparent increase of chemisorbed organic capping agents on the Ag surface depending on the character of additional ligand presented in the reaction environment.[1] The silver fraction for the pure carboxylate sample Ag-Pal exactly corresponds to that for nanoparticles obtained by the thermal decomposition method [17]. For the others the palmitate appears to be also the dominant capping agent which could not be totally removed or replaced by long chain amine or thiol, as confirmed by FTIR and DSC studies.

Figure 1 shows a TEM image of Ag-Pal nanoparticles, the average diameter of which is 4.5 ± 0.2 nm. Their polydispersity, small size, and regular shape is reflected in UV–Vis spectrum in cyclohexane, which presents almost symmetrical shape of plasmon resonance band with a maximum at 428 nm (Fig. 2). The same picture shows absorption spectra of colloids Ag-Pal/HDA and Ag-Pal/HDT exhibiting absorption maximum at 428 and 444 nm, respectively. No change in the plasmon band position in the presence of HDA as the second co-ligand indicates that HDA influences the resonance of free electrons in silver particles to a small extent. Contrary, the 16-nm red-shift for carboxylate/thiol caped NPs provides evidence for stronger interactions via bond formation on the silver surface with sulphur atom. This finding is consistent with the trend observed for ligand reactivity which showed that thiols are considerably stronger ligands than amines [33, 34].

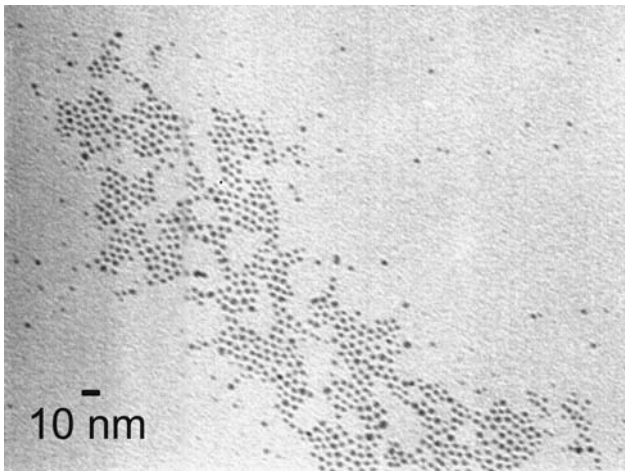

Fig. 1 Transmission electron micrograph (TEM) image of palmitate-stabilized silver nanoparticles Ag-Pal. The film was drop-cast by putting a drop of cyclohexane-dispersed Ag nanoparticles on carbon-coated copper grid

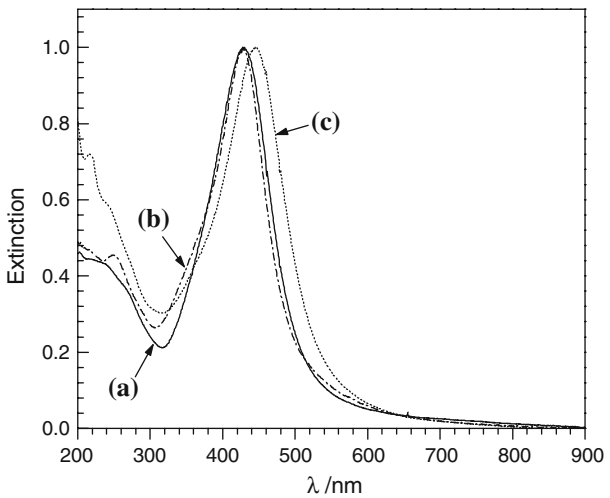

Fig. 2 UV–Vis absorption spectra of palmitate-capped Ag particles with various composition of protecting shell *a* pure palmitate, *b* palmitate/HDA, and *c* palmitate/HDT in cyclohexane

[1] The organic and metal mass values obtained from elemental analysis and TGA measurements do not sum to 100% but present systematic excess of about 3.5% which results from different analytical methodologies.

To examine the adsorption origin of the anchoring groups on silver nanocrystals formed as a result of hydrogen reduction of carboxylate, FTIR measurements were carried out on the pure palmitate protected silver NPs and on the composite palmitate/HDA and palmitate/HDT systems, and compared with the spectrum of silver palmitate precursor (Fig. 3). The spectra prove the presence of all the capping compounds at the surface. Alkane carboxylates form chelating bidentate bonding with Ag^+ [35, 36] and show characteristic asymmetrical stretching vibration at 1519 cm^{-1} ($\nu_{as}(COO^-)$) and symmetrical one at 1422 cm^{-1} ($\nu_s(COO^-)$). These important vibrational modes for the coordinative carboxylate group are also presented in the passivated silver nanoparticles, though their features and frequencies are significantly modified [37–39]. When bound to a metal surface an intense band at 1395 cm^{-1} appears, which is the red-shifted symmetric COO^- stretching mode. Its position clearly confirms a bridging bidentate binding of two carboxylate oxygens to silver. Two featureless and low intensity bands at 1548/1523 cm^{-1} we ascribed as a relict vibration of the asymmetrical $\nu_{as}(COO^-)$ stretch.

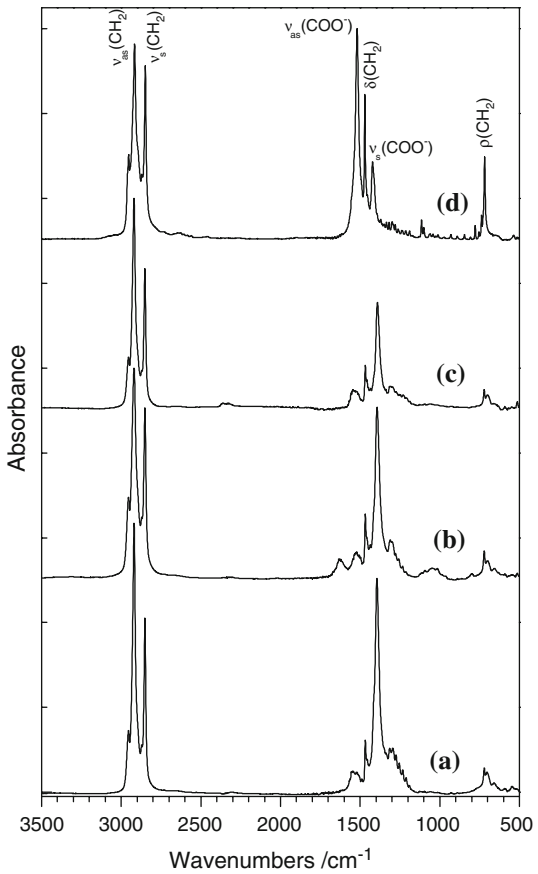

Fig. 3 FTIR spectra of *a* Ag-Pal, *b* Ag-Pal/HDA, *c* Ag-Pal/HDT, and *d* neat silver palmitate deposited from cyclohexane onto a Si support. Each spectrum was obtained by averaging 64 interferograms with resolution of 4 cm^{-1}

This would indicate that there are some sites on the Ag nanocrystal surface, probably at vertex or facet atoms, which form linkages with COO^- having still chelating bidentate and/or ionic character. Both bands reflect a complex stabilization activity of palmitate on Ag nanoparticles. The positions of the carboxylate COO^- stretching vibrations are not affected by the presence of another organic ligand in the composite capping shell. Although less intense relative to aliphatic CH_2 stretching bands (due to the increasing hydrocarbon coverage) they are visible at the same wavenumbers for all samples. The presence of hexadecylamine coordinated to the nanoparticle was identified by weak and broadened feature at 1627 cm^{-1} due to δ(N–H) bond deformation. Similarly to $\nu_{as}(COO^-)$ vibrations, $\nu(NH_2)$ stretching modes observed at 3332 and 3256 cm^{-1} for the neat HDA, are also strongly damped and almost absent in the spectrum of Ag-Pal/HDA. Such IR band suppression is often observed at metallic surfaces and results from the parallel alignment of the induced dipolar moment to the silver surface. These vibrational modes, O–C–O and H–N–H stretchings, according to the surface infrared selection rule are not active. The IR spectrum of the Ag-Pal/HDT nanoparticles and the neat HDT are similar to one another except of a remarkable difference in the peak intensity of methylene vibrations (vide infra). In the light of this, FTIR transmission spectra unambiguously show formation of the multicoated Ag nanoparticles. They also give the occasion to characterize the packing arrangement of the alkyl chains and their order with regard to vibrational modes of methylene units CH_2 [40–42]. For the three samples studied CH_2-band positions and shapes are the same. In the spectra, one can identify the asymmetric (2919 cm^{-1}) and symmetric (2850 cm^{-1}) stretching vibrations, scissoring (1467 cm^{-1}) and rocking bands (720 cm^{-1}). These vibrational modes reveal small yet important differences in band frequencies, intensities, and splitting relative to the neat carboxylate silver salt, HDA, HDT, or palmitic acid. They are mainly due to chain end conformation and chain-packing changes and can be explained on the basis of results discussed in detail earlier [40–42]. The stretching methylene modes, sensitive to conformation, are shifted by $\sim$3 cm^{-1} to higher frequencies. The lower position and reduced intensity of scissoring vibration peak at 1467 cm^{-1} can point to hexagonal packing of alkyl chains which assume a disordered conformation on NPs. Similarly, a higher position of strongly suppressed peak at 720 cm^{-1} indicates the existence of a number of internal kink defects [43]. Though the methylene modes support the less compact packing of alkane ligands on the silver surface making the adsorbed layer itself more fluid, the progression bands in the range of

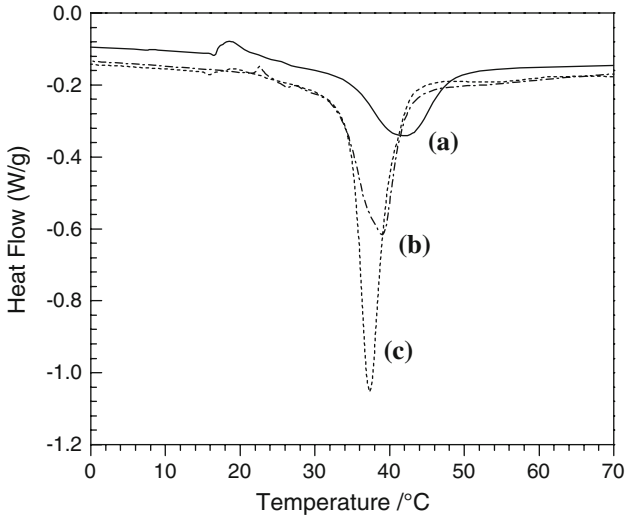

Fig. 4 DSC scans (10°/min) of *a* Ag-Pal, *b* Ag-Pal/HDA, and *c* Ag-Pal/HDT

1350–1150 cm^{-1} shows that the microenvironment of the monolayers is similar to that of bulky materials. This holds for the all coverings investigated here.

Powdered silver nanoparticle material was also analyzed by DSC to get information on the thermodynamics of the systems (Fig. 4). During thermal scanning the samples undergo clear endothermic transformations, position and enthalpy of which can be related to the composition and the amount of the coordinated ligand. DSC traces of pure palmitic acid, HDA, and HDT show sharp endothermal peaks with the melting temperature T_m at 62.5, 48.4 (the second at 82 °C) and 23.9 °C, respectively. The first endothermic transition for silver palmitate occurs at 116.0 °C. Ag-Pal, Ag-Pal/HDA, and Ag-Pal/HDT nanoparticles exhibit melting transition T_m at 41.7 ($\Delta H =$ 20.1 J/g), 39.0 ($\Delta H = 23.2$ J/g), and 37.4 °C ($\Delta H =$ 27.5 J/g), respectively. Thus, the melting temperatures are evidently lowered to that corresponding to pure ligands. It is also worth noticing that the phase transition temperature of Ag-Pal/HDT is lower than the value reported for pure Ag/thiolate clusters (~65 °C) [44]. DSC results reinforce the hypothesis that all passivating ligands are coordinated to the silver surface, which in turn imposes the packing of the aliphatic ligands and their cooperative arrangements. This observation supports also the view on higher reactivity of the silver nanoparticles surface relative to the analogous Au system.

Conclusions

We have described a versatile method for the synthesis of re-dispersible silver nanoparticles based on the carboxylate reduction under hydrogen pressure. This method is an alternative to the known high temperature thermolysis of silver carboxylates. It allows to receive silver nanoparticles in gram scale quantities in low-boiling solvents, while significantly reducing the reaction time. Also another stabilizing ligand can be employed during the synthesis such as hexadecylamine or hexadecanethiol. In the dual passivating system both amine and thiol were found to be tightly bounded to the silver nanoparticle surface. Although the second capping agent does not dictate stability of the silver colloid, it lowers the overall metal content in the nanomaterial, thus widening potentials for the effective surface functionalization. It was demonstrated that coordination with an additional ligand adjusts physicochemical properties of the nanoparticles. The high monodispersity of the obtained colloids and the variety of applied surfactants at mild reaction conditions, including functionalized carboxylates, amines and thiols, make the proposed synthesis attractive for numerous applications of silver nanoparticles in non-aqueous media.

References

1. Fleming DA, Williams ME (2000) Langmuir 20:3021
2. Hiramatsu H, Osterloh FE (2004) Chem Mater 16:2509
3. Brust M, Walker M, Bethell D, Schiffrin DJ, Whyman R (1994) Chem Commun 801
4. Leff DV, Ohara PC, Heath JR (1996) Langmuir 12:4723
5. Uznanski P, Amiens C, Chaudret B, Bryszewska E (2006) Pol J Chem 80:1845
6. Wang Y, Yang H (2006) Chem Commun 2545
7. Nakamoto M, Yamamoto M, Fukusumi M (2002) Chem Commun 1622
8. Green M, Allsop N, Wakefield G, Dobson PJ, Hutchison JL (2002) J Mater Chem 12:2671
9. Wang W, Chen X, Efrima S (1999) J Phys Chem 103:7238
10. Zamborini FP, Gross SM, Murray RW (2001) Langmuir 17:481
11. Quiros I, Yamada M, Kubo K, Mizutani J, Kurihara M, Nishihara H (2002) Langmuir 18:1413
12. Pan Ch, Pelzer K, Philippot K, Chaudret B, Dassenoy F, Lecante P, Casanove M-J (2001) J Am Chem Soc 123:7584
13. Wu N, Fu L, Su M, Aslam M, Wong KCh, Dravid VP (2004) Nano Lett 4:383
14. Lacroix L-M, Lachaize S, Falqui A, Respaud M, Chaudret B (2009) J Am Chem Soc 131:549
15. Cordente N, Respaud M, Senocq F, Casanove M-J, Amiens C, Chaudret B (2001) Nano Lett 1:565
16. Fields EK, Meyerson S (1976) J Org Chem 4:916
17. Abe K, Hanada T, Yoshida Y, Tanigaki N, Takiguchi H, Nagasawa H, Nakamoto M, Yamaguchi T, Yase K (1998) Thin Solid Films 327–329:524
18. Yamamoto M, Nakamoto M (2003) J Mater Chem 13:2064
19. Kashiwagi Y, Yamamoto M, Nakamoto M (2006) J Colloid Interface Sci 300:169
20. Yamamoto M, Kashiwagi Y, Nakamoto M (2006) Langmuir 22:8581
21. Wu YL, Li YN, Ong BS (2006) J Am Chem Soc 128:4202
22. Hendriks CE, Smith PJ, Perelaer J, Van den Berg AMJ, Schubert US (2008) Adv Funct Mat 18:1031

23. Shim IK, Lee YI, Lee KJ, Joung J (2008) Mater Chem Phys 110:316
24. Ahn BY, Duoss EB, Motala MJ, Guo X, Park S-I, Xiong Y, Yoon J, Nuzzo RG, Rogers JA, Lewis JA (2009) Science 323:1590
25. Khanna PK, Kulkarni D, Beri RK (2008) J Nanopart Res 10:1059
26. Shim IK, Lee YI, Lee KJ, Joung J (2008) Mater Chem Phys 110:316
27. Ryu BH, Choi Y, Park H-S, Byun J-H, Kong K, Lee J-O, Chang H (2008) Colloids Surf A 270–271:345
28. Amiens C, Chaudret B (2007) Mod Phys Lett B 21:1133
29. Wang TC, Rubner MF, Cohen RE (2002) Langmuir 18:3370
30. Evanoff DD Jr, Chumanov G (2004) J Phys Chem B 108:13948
31. Steffan M, Jakob A, Claus P, Lang H (2009) Catal Commun 437
32. Yoon S, Kwon WJ, Piao L, Kim SH (2007) Langmuir 23:8295
33. He ST, Yao JN, Jiang P, Shi DX, Zhang HX, Xie SS, Pang SJ, Gao HJ (2001) Langmuir 17:1571
34. Malinsky MD, Kelly KL, Schatz GC, Van Duyne RP (2001) J Am Chem Soc 123:1471
35. Nara M, Torii H, Tasumi M (1996) J Phys Chem B 100:19812
36. Weichold O, Hsu SC, Moller M (2006) J Mater Chem 16:4475
37. Lee SJH, WCh Sang, Hyouk J, Kim K (2002) J Phys Chem B 106:2892
38. Kariuki NN, Luo J, Hassan SA, Lim IIS, Wang LY, Zhong CJ (2006) Chem Mater 18:123
39. Tao YT (1993) J Am Chem Soc 115:4350
40. Tao YT, Huang CY, Chiou DR, Chen LJ (2002) Langmuir 18:8400
41. Parikh AN, Gillmor SD, Beers JD, Beardmore KM, Cutts RW, Swanson BI (1999) J Phys Chem B 103:2850
42. Ulman A (1996) Chem Rev 96:1533
43. Li H-W, Strauss HL, Snyder RG (2004) J Phys Chem B 108:6629
44. Sandhyarani N, Antony MP, Panneer Selvam G, Pradeep T (2000) J Chem Phys 113:9794